Anthropogenic Aerosols and the Weakening of the South Asian Summer Monsoon

Massimo A. Bollasina,[1] Yi Ming,[2]* V. Ramaswamy[2]

Observations show that South Asia underwent a widespread summertime drying during the second half of the 20th century, but it is unclear whether this trend was due to natural variations or human activities. We used a series of climate model experiments to investigate the South Asian monsoon response to natural and anthropogenic forcings. We find that the observed precipitation decrease can be attributed mainly to human-influenced aerosol emissions. The drying is a robust outcome of a slowdown of the tropical meridional overturning circulation, which compensates for the aerosol-induced energy imbalance between the Northern and Southern Hemispheres. These results provide compelling evidence of the prominent role of aerosols in shaping regional climate change over South Asia.

The South Asian summer monsoon provides up to 80% of the annual mean precipitation for most regions of India and has tremendous impacts on agriculture, health, water resources, economies, and ecosystems throughout South Asia (*1*). It is also an important part of the global-scale atmospheric circulation, because its vigorous ascent dominates the boreal summer tropical meridional overturning (the Hadley circulation) (*2*) and has profound remote influences (*3*). A possible long-term (decadal to centennial) shift in monsoon rainfall associated with climate change could have even more far-reaching consequences for the region than do natural variations. A number of observational studies have investigated the multidecadal trend of monsoon rainfall over India and found a persistent drying trend during the second half of the 20th century (*4*–*7*). Yet the root cause of this trend remains unclear.

Both aerosols and greenhouse gases can affect the South Asian summer monsoon. The increase of aerosols and associated decrease in surface solar radiation ("dimming") over South Asia have been well documented (*4*, *8*). Climate model experiments suggested that sulfate aerosol may significantly reduce monsoon precipitation (*9*). Recent studies, some of which focused specifically on absorbing aerosols (*4*, *8*, *10*, *11*), postulate as possible mechanisms both surface cooling from reduced surface solar radiation [and consequent reduction of the meridional thermal contrast between the northern and southern Indian Ocean (*5*)] and atmospheric heating due to absorption of solar radiation (*8*).

The warming caused by increased greenhouse gases, meanwhile, may also play a role. Annual mean tropical sea surface temperatures (SSTs) have increased by ~0.5 K since the 1950s. This warming is particularly notable over the Indian Ocean (*12*). Tropical circulation (particularly its zonal component) is expected to weaken in response to an increase in surface temperature, because global mean precipitation, which is controlled by the overall atmospheric energy balance, cannot increase as fast as the lower tropospheric water vapor concentration (the thermodynamical scaling argument) (*13*, *14*). Despite a weakening of the monsoon circulation, most studies project an increase of the seasonal monsoon rainfall under global warming, partly owing to more abundant water vapor (*15*).

We used several long-term observational data sets of precipitation to identify possible recent trends in the South Asian monsoon (*16*). The boreal summer (June to September) climatological precipitation has a widespread maximum over central-northern India, which includes part of the vastly irrigated and socially important Indo-Gangetic Plain. Our initial focus is on this analysis region (76° to 87°E, 20° to 28°N), whose location and size are similar to those in (*17*). The Climate Research Unit (CRU) data show a marked reduction from the 1950s to the end of the 20th century (Fig. 1). The linear trend of -0.95 mm day^{-1} (50 $years)^{-1}$ is statistically significant at the 95% confidence level ($P = 0.04$) (*18*). Comparable drying trends are also seen in the University of Delaware (UDEL) and global 50-year precipitation reconstruction analysis (PREC/L) data sets. This finding is broadly consistent with previous studies (*5*, *7*, *19*, *20*), which made use of additional data sets. Although the Indian Meteorological Department (IMR) data show a small downward trend, it is not statistically significant enough. The decrease amounts to 9 to 11% of the total monsoon rainfall received by the region for CRU, UDEL, and PREC/L, and 2% for IMR [fig. S4 and supporting online material (SOM)].

Even more interestingly, a coherent large-scale pattern emerges: a drying over central-northern India and most of Southeast Asia (consisting of Indochina and the Maritime Continent), coinciding with a slight wettening over southern India and over northwestern India and Pakistan (Fig. 2). This distinct spatial structure is consistent among the majority of the data sets (fig. S5 and SOM). Averaged over the whole country, the Indian summer rainfall underwent a reduction of 4 to 5% over 50 years (*4*, *6*, *7*).

Was this observed change of the South Asian monsoon precipitation caused by natural variability or human interference? If the latter, what were the relative contributions of aerosols and

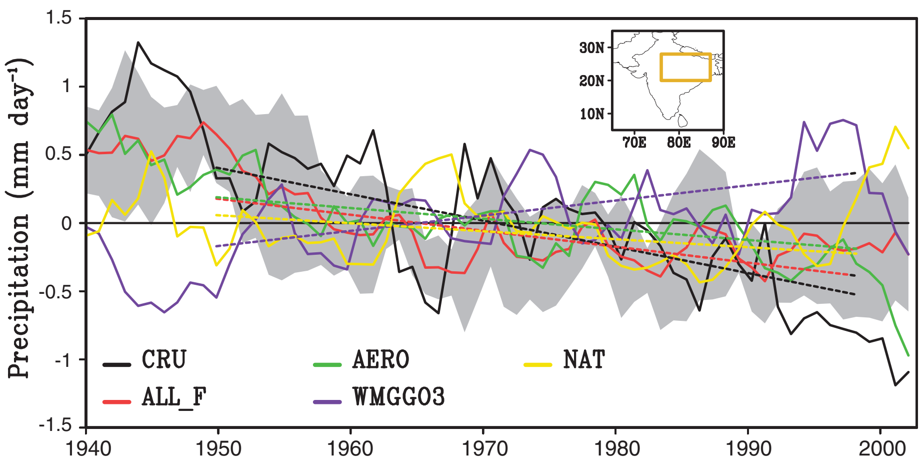

Fig. 1. Five-year running mean June-September average precipitation anomalies over central-northern India (76° to 87°E, 20° to 28°N; see the orange box in the inset map). Anomalies are calculated as deviations from the 1940–2005 climatology. The black line is based on the CRU TS 3.0 observational data set. The red, green, blue, and yellow lines are for the ensemble-mean all-forcing (ALL_F), aerosol-only (AERO), greenhouse gases and ozone-only (WMGGO3), and natural forcing-only (NAT) CM3 historical integrations, respectively. The gray shading represents the standard deviation of the five-member all-forcing ensemble. The least-squares linear trends during 1950–1999 are plotted as dashed lines in the respective colors. The trend [mm day^{-1} (50 $years)^{-1}$] and its P value based on the two-tailed Student's t test (*32*) (in parentheses) are as follows: −0.95 ($P = 0.04$) for CRU, −0.58 ($P = 0.01$) for ALL_F, −0.39 ($P = 0.09$) for AERO, 0.55 ($P = 0.07$) for WMGGO3, and −0.29 ($P = 0.17$) for NAT. The 50-year trends from the other three observational data sets, which are not plotted to avoid overcrowding the figure, are −0.20 ($P = 0.70$) for IMR, −0.79 ($P = 0.10$) for UDEL, and −0.76 ($P = 0.10$) for PREC/L.

[1]Program in Atmospheric and Oceanic Sciences, Princeton University, Princeton, NJ 08542, USA. [2]Geophysical Fluid Dynamics Laboratory/National Oceanic and Atmospheric Administration, Princeton, NJ 08542, USA.

*To whom correspondence should be addressed. E-mail: Yi.Ming@noaa.gov

greenhouse gases, the two most important anthropogenic climate-forcing agents? Answering these questions poses a challenging test case for our fundamental understanding of the core working of Earth's hydrological cycle, and it holds the key to a more reliable projection of regional climate change.

Ensemble simulations with a state-of-the-art coupled atmosphere-ocean global climate model (GCM) provide us a means to attribute the observed long-term trend. The model we used is the U.S. National Oceanic and Atmospheric Administration (NOAA) Geophysical Fluid Dynamics Laboratory (GFDL) CM3 GCM, which includes an explicit treatment of the aerosol-cloud interactions and aerosol indirect effects (*21*). The model data analyzed in this study cover the period 1951–1999 and come mainly from three sets of historical simulations (1860–2005): (i) a five-member ensemble with all of the forcings, natural (solar variations and volcanoes) and anthropogenic (well-mixed greenhouse gases, ozone, aerosols, and land use) alike (ALL_F); (ii) a three-member ensemble with greenhouse gases and ozone forcings only (WMGGO3); and (iii) a three-member ensemble with aerosol forcing only (AERO). The ensemble simulations forced with all of the natural forcings only (NAT) and with all of the anthropogenic forcings only (ANTHRO) were also examined (SOM).

The all-forcing ensemble (ALL_F) captures the drying trend over central-northern India reasonably well (Fig. 1). The simulated large-scale drying over the eastern equatorial Indian Ocean and Bay of Bengal appears to be consistent with the observed pattern over the adjacent lands (such as the west coast of Indochina) (Fig. 2). The model also projects wetter conditions over the western equatorial Indian Ocean and northern Arabian Sea. The latter is in agreement with the observed moistening over Pakistan. The drying over central-northern India is likely to be of anthropogenic origin, because the mean trend of the naturally forced ensemble is too weak to reproduce the observed pattern (figs. S6 and S7 and SOM). Deficiencies in simulating the radiative-dynamical interaction of the monsoon flow with the elevated orography of the Tibetan Plateau, owing to the model's relatively coarse horizontal resolution, are likely to be responsible for the substantial disagreement over southern China.

The individual ensembles forced with different forcing combinations clearly indicate that the drying over central-northern India can be attributed to aerosols (AERO) (Fig. 1). The region would become wetter if the model were driven only by greenhouse gases and ozone (WMGGO3). WMGGO3 appears to amplify the trend in AERO, indicating nonlinearity in the total response to both forcings (*22*, *23*). These findings are also

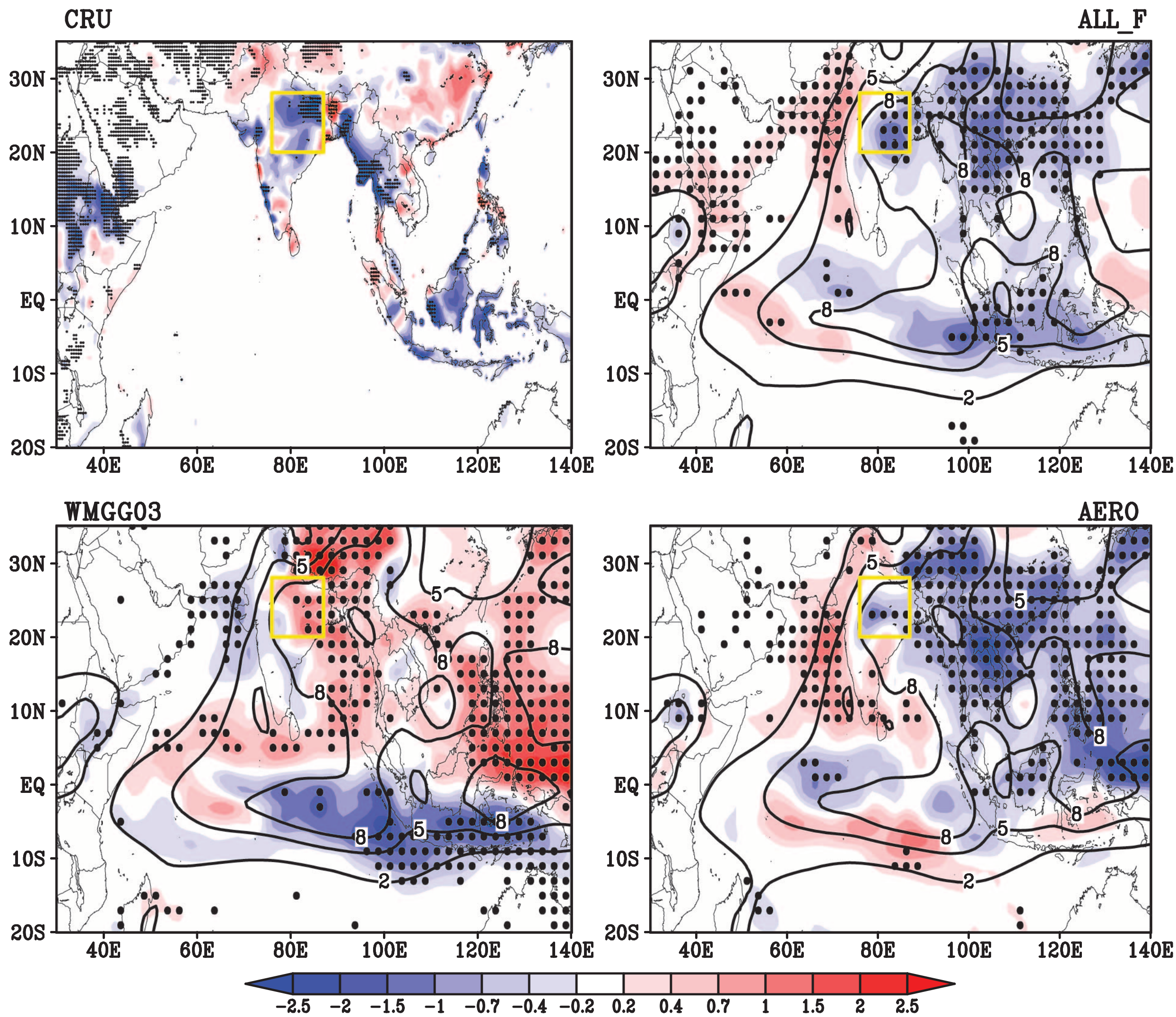

Fig. 2. Spatial patterns of the 1950–1999 least-squares linear trends of the June-September average precipitation [mm day^{-1} (50 years)$^{-1}$]. The panels are for the CRU TS 3.0 observational data set and the ensemble-mean all-forcing (ALL_F), aerosol-only (AERO), greenhouse gases and ozone-only (WMGGO3) CM3 historical integrations. The black dots mark the grid points for which the trend exceeds the 95% significance level ($P < 0.05$) according to the two-tailed Student's t test (*32*). For the model simulations, the black contour lines represent the 1946–1955 average precipitation (mm day^{-1}). The orange boxes denote the area of averaging for central-northern India used in Fig. 1.

supported by the results based on the analysis box of (*17*) (SOM). Aerosols (AERO) also appear responsible for the changes in the latitudinal direction over Southeast Asia in the all-forcing ensemble (Fig. 2). The reduced precipitation over northern India, Indochina, and southern China is accompanied by weaker ascent (fig. S8). The anomalous subsiding flow moves southward and then starts to converge in the equatorial region, closing the meridional cell (fig. S9) and enhancing local precipitation (Fig. 2). This circulation change opposes the regional climatological meridional overturning.

On the other hand, the impact of greenhouse gases and ozone (WMGGO3) is more pronounced around the equator. The main features are the widespread anomalous subsidence over the Maritime Continent and the eastern Indian Ocean, and the enhancement of ascent over the western Pacific to a similar extent (fig. S8). This zonal dipole pattern is indicative of an eastward shift of the convergence zone. This relatively localized change is accompanied by a weakening of the basin-wide equatorial zonal circulation (*12*, *13*). Greenhouse gases and ozone also cause the meridional overturning circulation over South Asia and Southeast Asia to slow down, albeit slightly (fig. S9). The large equatorial subsidence seen in fig. S9 arises from the decreased ascent over the eastern Indian Ocean (fig. S8), which is largely part of the zonal adjustment. Aerosol-induced changes are almost opposite along the equator. Ascent is reduced over the western Pacific but is intensified over the Indian Ocean, giving rise to a westward movement of the convergence zone. This is in addition to a modest strengthening of the zonal circulation.

The impacts of aerosols and greenhouse gases simulated in these GCM experiments can be understood theoretically by separating the tropical circulation adjustment to radiative forcing into its thermodynamical (i.e., due to changes in temperature and atmospheric moisture content) and dynamical (i.e., due to circulation changes caused by nonthermodynamical factors) components (Fig. 3). The former complies with the thermodynamical scaling argument, which dictates that in a warmer climate (such as under greenhouse gas forcing), the overall circulation will weaken despite an increase in total precipitation, and vice versa (*12–14*, *23–25*). In other words, the thermodynamically induced circulation change scales approximately with the variation in the tropical mean surface temperature, regardless of the specificities of the underlying forcing (figs. S10 and S11 and SOM). The change is manifest mostly in the zonal component of the tropical circulation, which is less constrained than its meridional counterpart (*13*, *23*). In stark contrast, a spatially inhomogeneous forcing (such as aerosol forcing) is much more efficient in causing a dynamically induced circulation change, as the coupled atmosphere-ocean system adjusts circulation to compensate for the energy imbalance between the region under the direct influence of the forcing and its surroundings. In doing so, the impact of the forcing (the change in surface temperature) due to the spatial asymmetry spreads beyond its boundaries (*22*, *26*). Because anthropogenic aerosols are located mainly in the Northern Hemisphere, the boreal summer meridional circulation, of which the South Asian summer monsoon is a major part (*2*), weakens to reduce the energy flow to the Southern Hemisphere and thus partially alleviates the interhemispheric asymmetry due to aerosol forcing (figs. S13 and S14 and SOM). Although this theory can help explain some of the main characteristics of the model simulations and is consistent with the observed reduction in the South Asian monsoon rainfall, the extent to which it holds for the real climate still needs to be assessed carefully with more observations, especially in light of the disagreement about southern China.

The lower tropospheric stability in AERO shows no appreciable change over central-northern India in May, indicating that absorbing aerosols probably play a very limited, if any, role in affecting the multidecadal trend of the monsoon through modulating the atmospheric stability (fig. S15 and SOM). This, however, does not mean that absorbing aerosols cannot exert substantial influence on the monsoon at shorter time scales (such as interannual scales). The aerosol-induced differential cooling of the source and nonsource regions, which is realized mainly through indirect effects, is effective in reducing not only the local land-ocean surface thermal contrast, but also the large-scale meridional atmospheric temperature and sea level pressure (SLP) gradients (figs. S11 and S17 and SOM). These adjustments are the physical mechanisms behind the weakening of the South Asian monsoon, which can be viewed approximately as part of the slowdown of the tropics-wide meridional overturning circulation.

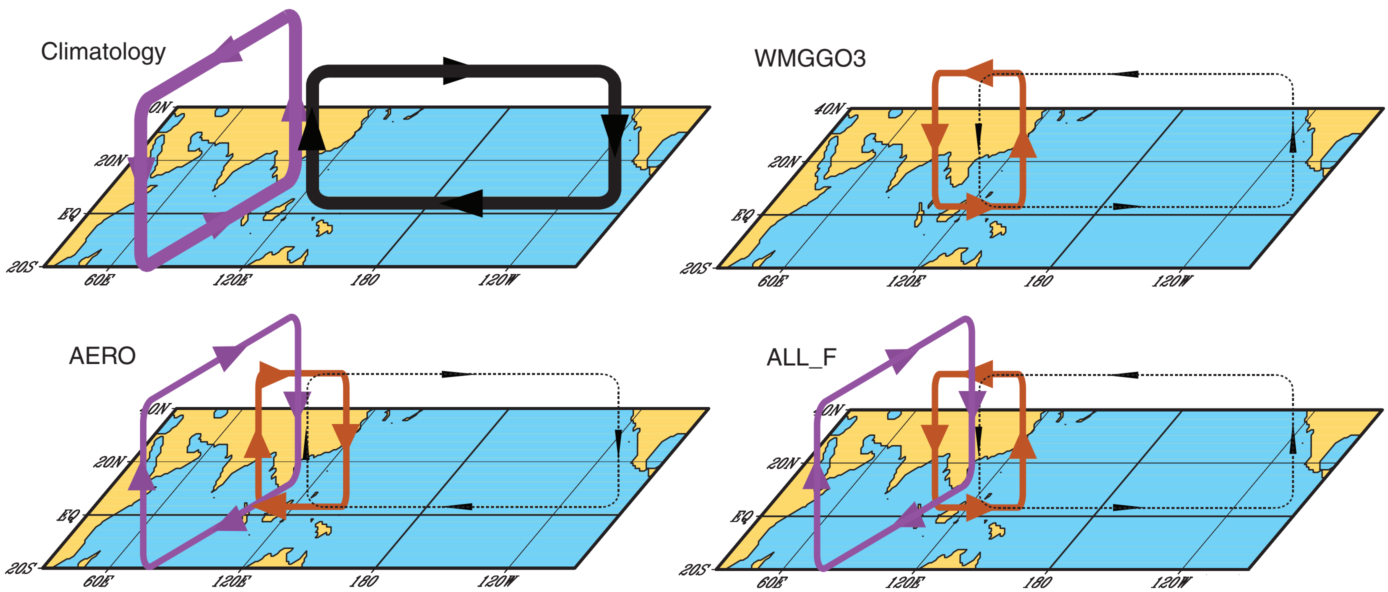

Fig. 3. Schematic of the large-scale circulation changes caused by greenhouse gases and aerosols. The warming caused by greenhouse gases and ozone (WMGGO3) induces a strong anomalous zonal circulation (red) between the eastern Indian Ocean (weaker ascent) and the western Pacific (stronger ascent), in addition to a modest weakening of the equatorial zonal circulation (black). Aerosols (AERO) are responsible for an anomalous meridional circulation, which reduces the ascent over the western Pacific and Southeast Asia (purple) and opposes the local Hadley circulation. Besides, the aerosol-induced cooling excites a strong anomalous zonal circulation (red), with stronger ascent over the eastern Indian Ocean and weaker ascent to the east, and strengthens the equatorial zonal circulation (black). The circulation changes in the all-forcing case (ALL_F) result from the overall warming (which is predominant in the longitudinal direction along the equator) and aerosol forcing (which outweighs the warming in the latitudinal direction). A conceptual representation of the climatological circulation is provided for reference.

This work is distinct from the recent studies with fully coupled climate models (*4*, *10*) in a number of aspects. For instance, the all-forcing experiments we performed substantially advance the ability to simulate the observed drying over central-northern India (*10*). Another study is able to achieve this, but with the aerosol forcing over South Asia and the tropical Indian Ocean constrained by observations (*4*). The representation of aerosol physics in the present model is substantially enhanced as compared with earlier studies. The main improvements include aerosols being interactive with the meteorology, internal mixing, and indirect effects. This approach to aerosol modeling is more suitable for projecting future climate change than the approaches used earlier (*4*, *8*), and it is expected that it improves the realism of the simulated forcing pattern. In this model, aerosols interact with the monsoon circulation largely by altering clouds (the indirect effects), with other factors such as atmospheric stability changes owing to absorbing aerosols playing a much lesser role, whereas the previous studies (*4*, *8*) were devoted to understanding how aerosols affect clear-sky radiation and atmospheric stability (the direct effects). The observed change in the meridional SST gradient over the Indian Ocean was attributed to the unevenly distributed local aerosol forcing and was postulated to be responsible for the weaker monsoon circulation (*4*, *5*). By raising the possibility that the internal feedbacks of the climate system are more influential than the spatial pattern of aerosol forcing in affecting the SST gradient over the western part of the Indian Ocean, this study emphasizes the differential cooling of the source and nonsource regions and the reduction in the land-ocean surface thermal contrast as the main mechanisms of the weakening of the monsoon circulation.

On the theoretical side, we consider the drying fundamentally as part of the global-scale circulation adjustment to an asymmetrical forcing (*23*, *26*), as opposed to the joint result of a number of regional factors (*4*). An implication of this more expanded view is that nonlocal aerosol forcing may also affect the South Asian monsoon. Furthermore, the successful decomposition of the overall circulation change into those in the zonal and meridional components of the tropical circulation provides a useful framework for understanding the combined climate response to aerosols and greenhouse gases.

The results discussed here suggest that anthropogenic aerosols have substantially masked the precipitation increase over the monsoon area that would otherwise have occurred purely in response to increased greenhouse gases, and they imply that future aerosol emissions are important controlling factors of near-term regional climate change. The outcomes of this study, especially the realistic simulation and theoretical understanding of Asian regional precipitation variations, constitute a concrete step toward unraveling the hydrological impacts of climate change at even finer scales.

References and Notes

1. P. J. Webster *et al.*, *J. Geophys. Res.* **103**, 14451 (1998).
2. K. E. Trenberth, J. W. Hurrell, D. P. Stepaniak, in *The Asian Monsoon*, B. Wang, Ed. (Springer/Praxis Publishing, New York, 2006), pp. 417–457.
3. Z. Peiqun, S. Yang, V. E. Kousky, *Adv. Atmos. Sci.* **22**, 915 (2005).
4. V. Ramanathan *et al.*, *Proc. Natl. Acad. Sci. U.S.A.* **102**, 5326 (2005).
5. C. E. Chung, V. Ramanathan, *J. Clim.* **19**, 2036 (2006).
6. S. Gadgil, K. R. Kumar, in *The Asian Monsoon*, B. Wang, Ed. (Springer/Praxis, New York, 2006), pp. 651–682.
7. K.-M. Lau, K.-M. Kim, *Geophys. Res. Lett.* **37**, L16705 (2010).
8. K.-M. Lau, K.-M. Kim, *Geophys. Res. Lett.* **33**, L21810 (2006).
9. J. F. B. Mitchell, T. C. Johns, *J. Clim.* **10**, 245 (1997).
10. G. A. Meehl, J. M. Arblaster, W. D. Collins, *J. Clim.* **21**, 2869 (2008).
11. C. Wang, D. Kim, A. M. L. Ekman, M. C. Barth, P. J. Rasch, *Geophys. Res. Lett.* **36**, L21704 (2009).
12. G. A. Vecchi, B. J. Soden, *J. Clim.* **20**, 4316 (2007).
13. I. M. Held, B. J. Soden, *J. Clim.* **19**, 5686 (2006).
14. G. A. Vecchi *et al.*, *Nature* **441**, 73 (2006).
15. H. Ueda, A. Iwai, K. Kuwako, M. E. Hori, *Geophys. Res. Lett.* **33**, L06703 (2006).
16. Long-term observations of precipitation and SLP were used in this study. In order to account for the different sources of measured precipitation and methodologies, four precipitation data sets were considered: the CRU TS3.0 data set (*27*), the IMR 1951–2003 high-resolution daily data set for the Indian region (*28*), the UDEL 1900–2008 gridded monthly time series of terrestrial precipitation (Version 2.01) (*29*), and the global 50-year PREC/L (*30*). The Hadley Centre HadSLP2 SLP data set (*31*) was used to infer the long-term changes in the tropical circulation (figs. S5 and S11 and SOM).
17. B. N. Goswami, V. Venugopal, D. Sengupta, M. S. Madhusoodanan, P. K. Xavier, *Science* **314**, 1442 (2006).
18. Two methods were used to estimate the statistical significance of the linear trends. The first one is based on the two-tailed Student's *t* test (*32*), in which the variance of the residuals is used to estimate the standard error of an observed or simulated trend. It is applied both to the average precipitation over central-northern India (Fig. 1) and to individual grid points (Fig. 2). By constructing the probability distribution of natural trends from an 800-year control simulation either for a single realization or for a multimember ensemble, we can also determine the probability of a trend occurring in the absence of external forcings (figs. S3 and S4 and SOM).
19. B. Wang, Q. Ding, *Geophys. Res. Lett.* **33**, L06711 (2006).
20. L. Zhang, T. Zhou, *Clim. Dyn.* **37**, 279 (2011).
21. The NOAA GFDL CM3 GCM (*33*) implements an improved representation of aerosol effects, including the indirect ones involving liquid clouds. Sulfate, organic carbon, and sea salt aerosols act as cloud condensation nuclei. Possible aerosol effects on ice clouds are not included. The horizontal resolution is ~200 km. Approximately half of the 48 vertical layers reside in the troposphere, and the vertical resolution is ~70 m near the surface and ~1 km near the tropopause. These resolutions are comparable to those of most of the current GCMs used for attribution studies. The model-simulated climatological monsoon winds and precipitation compare reasonably well with observations (fig. S2). The orography-related subregional features (such as the rain-shadow effect over southeast India and the spatial pattern of precipitation over central-northern India and along the Himalayas) are also simulated realistically. See SOM for more detail.
22. Y. Ming, V. Ramaswamy, *J. Clim.* **22**, 1329 (2009).
23. Y. Ming, V. Ramaswamy, *J. Clim.* **24**, 5125 (2011).
24. R. Seager, N. Naik, G. A. Vecchi, *J. Clim.* **23**, 4651 (2010).
25. M. Zhang, H. Song, *Geophys. Res. Lett.* **33**, L12701 (2006).
26. C.-T. Chen, V. Ramaswamy, *J. Clim.* **9**, 2788 (1996).
27. T. D. Mitchell, P. D. Jones, *Int. J. Climatol.* **25**, 693 (2005).
28. M. Rajeevan, J. Bhate, J. D. Kale, B. Lal, *Curr. Sci.* **91**, 296 (2006).
29. The data are archived online at http://climate.geog.udel.edu/~climate/html_pages/Global2_Ts_2009/README.global_p_ts_2009.html.
30. M. Chen, P. Xie, J. E. Janowiak, P. A. Arkin, *J. Hydrometeorol.* **3**, 249 (2002).
31. R. Allan, T. Ansell, *J. Clim.* **19**, 5816 (2006).
32. W. Woodward, H. Gray, *J. Clim.* **6**, 953 (1993).
33. L. J. Donner *et al.*, *J. Clim.* **24**, 3484 (2011).

Acknowledgments: We thank I. Held and G. Lau for reviewing an earlier version of the paper. The comments from two anonymous reviewers are also greatly appreciated.

Supporting Online Material
www.sciencemag.org/cgi/content/full/science.1204994/DC1
SOM Text
Figs. S1 to S17
References

1 March 2011; accepted 15 September 2011
Published online 29 September 2011;
10.1126/science.1204994

Increasing N Abundance in the Northwestern Pacific Ocean Due to Atmospheric Nitrogen Deposition

Tae-Wook Kim,[1] Kitack Lee,[1]* Raymond G. Najjar,[2] Hee-Dong Jeong,[3] Hae Jin Jeong[4]

The relative abundance of nitrate (N) over phosphorus (P) has increased over the period since 1980 in the marginal seas bordering the northwestern Pacific Ocean, located downstream of the populated and industrialized Asian continent. The increase in N availability within the study area was mainly driven by increasing N concentrations and was most likely due to deposition of pollutant nitrogen from atmospheric sources. Atmospheric nitrogen deposition had a high temporal correlation with N availability in the study area (*r* = 0.74 to 0.88), except in selected areas wherein riverine nitrogen load may be of equal importance. The increase in N availability caused by atmospheric deposition and riverine input has switched extensive parts of the study area from being N-limited to P-limited.

Rapid growth in human population and industrial activity has led to increases in the concentrations of pollutant nitrogen species (NO_x and NH_y) throughout the environment (*1*). However, the changes that result from anthropogenic nitrogen (air-N^{ANTH}) deposition into lakes and oceans have yet to be fully explored (*2*–*4*). Several recent studies have reported that the impacts of air-N^{ANTH} deposition on lakes and oceans can be locally substantial (*5*–*8*). For